Investigation of Low-grade Thermal Energy Harvesting using an Aqueous-based Thermoelectrochemical System

by

Chao Xu

Undergraduate Research Thesis
Submitted to the
Department of Mechanical and Aerospace Engineering
in Partial Fulfillment of the Requirements for the Degree of

Bachelor of Science in Mechanical Engineering
with Honor Research Distinction

at the

Ohio State University
Columbus, Ohio

April 2015

Oral Defense Committee Members:
Prof. Joseph Heremans, Advisor
Prof. Anne Co, Co-advisor
Prof. Yann Guezennec, Oral defense committee

Abstract

Improved efficiency of energy systems and development of sustainable, low-carbon-emission energy generation processes are essential for the long-term health of the environment as well as our economic, social and societal endeavors. Heat engines are typically 30% to 55% efficient, and loss roughly 15 terawatts energy in the form of waste heat to the environment.

Classical solid-state thermoelectric generators potentially provide an approach to improve the efficiency of those systems by converting waste heat directly into useful electricity, but have limited applications due to their high cost low and energy conversion efficiency.

In our research, we invented a liquid-state thermoelectrochemical cell. Based on ambipolar thermoelectric ion transport due to concentration difference in the water, ECTEGs can generate electric power in a temperature gradient from an electrolyte in which anions and cations have very different ions' mobilities. If the two types of ions have different mobilities in water solutions, the passage of cations with larger mobility can produce higher internal voltage than that of anions with less mobility. This produces a net internal voltage in the presence of a temperature gradient, without depleting the electrolyte chemically.

We present a quantitative theory for the effect and proved this principle by constructing an thermoelectrochemical cell with HNO3 and Ba(NO3)2 (hydrogen has a much larger mobility than other ions). The system was placed in temperature gradients and according to Le Chatelier's principle, adding to or removing heat from a reaction (HNO3 with Ba(NO3)2 in our research) can change the chemical equilibrium and thus the hydrogen concentration at different temperatures.

The output voltage is measured as function of temperature gradient, and the thermoelectrochemical cell produced - 903$\mu V/K$, experimentally. We also did a theoretical thermopower calculation for the cell with HNO3 and Ba(NO3)2 which is - 498 $\mu V/K$. The ZT of this thermoelectrochemical cell at 42.5 ℃ is about 0.013.

This thesis is dedicated to my parents
For their endless love, support and encouragement in all my pursuits

Acknowledgements

There are no proper words to convey my deep gratitude and respect for my thesis and research advisors, Professor Joseph Heremans and Professor Anne Co. I am only able to accomplish my first research thesis with their aspiration in and devotion to science, research and education, and with their patience, guidance and persistent help. A special thanks goes to Professor Yann Guezennec for his presence as my oral defense committee.

I would like to thank Professor Joseph Heremans for giving me this brilliant research idea and opportunity, helping me further my knowledge to the field of heat transfer physic and thermoelectric effect, and providing invaluable guidelines and advices for my research project and undergraduate studies. I also want to appreciate on the stimulating intellectual discussions and inspirations from Professor Anne Co which enrich my knowledge in the area of electrochemistry, and improve my capability to conceive my own research experiments and measurements.

Besides my research advisors, dozens of people have helped me immensely during this research project. First, I wish to thank both graduate students in Thermal Materials Laboratory and Co Research Laboratory. I especially praise the enormous amount of support by Dr. Yibin Gao, Dr. Richard Lei, and Bin He from Thermal Materials Laboratory, and also Josh Billy, Eric Coleman and Danny Liu from Co Research Group, and Senior Scientific Glassblower, Timothy Henthorne, from the Scientific Glassblowing Lab as well.

I gratefully acknowledge the funding sources that made my undergraduate research project possible. I was funded by the Office of Undergraduate Education at Ohio State University for my 2014 Summer Research Fellowship and was honored to receive undergraduate research scholarship from the College of Engineering at Ohio State University. My work was also supported by the Mechanical and Aerospace Engineering Department at Ohio State University.

A special thanks goes to my best friends at Ohio State University, Jason Jia and Yunli Chen, for all of those incredible memories we shared with each other and for all of those difficulties we went through with each other. They were always being supportive in any way they could.

Chao Xu

Ohio State University

April 2015

Table of Contents

List of Figures

List of Tables

Nomenclature

α	Seebeck coefficient or thermopower ($\mu V/K$)
β	effective ions mobility ration
η_{max}	Carnot efficiency
σ	electrical conductivity (mS/cm)
ρ	electrical resistivity (mΩ/cm)
λ	thermal conductivity (W/m-K)
μ	electrochemical potential (V)
A	Avogadro constant (6.022e23 /mol)
C_v	specific heat (kJ/kg)
e	magnitude of electron charge (-1.602e-19 C)
E	electric field (V/m)
j	electric density (A/m^2)
j_q	heat flux (W/m^2)
K_a	acid dissociation constant
k_B	Boltzmann constant (1.380e-23 J/K)
K_{sp}	solubility constant
M	molarity of solution (M)
n_-	concentration of anions (M)
n_+	concentration of cations (M)
pH	acidity and proton concentration measurement
S	entropy (kJ/K-kg)
u	ions mobility (cm^2/V-s)
U	internal energy (kJ)
z	ionization state of each ion
T_{cold}	cold side temperature of a thermoelectric couple (K)
T_{hot}	hot side temperature of a thermoelectric couple (K)
ΔT	temperature difference (K)
ΔV	voltage difference (V)
ZT	dimensionless thermoelectric figure of merit

Chapter 1: Introduction

1.1 Brief Current Energy Situation and Introduction to Waste Heat

Improved efficiency of energy systems and development of sustainable, low-carbon-emission energy generation processes are essential for the long-term health of the environment as well as our economic, social and societal endeavors. Variant renewable energy technologies and sources are under developing, which include battery-based electrification, decarbonizing fossil-fuel emissions and solar, wind, nuclear, geothermal, hydro and biomass, to generate clean and affordable electricity and energy, and improve overall national energy security. All of these technologies and energy sources present their own challenges and opportunities as a potential approach for sustainable energy future [1]. Among such a broad energy generating technologies, this research project's main objective is to develop a new theory or technology which focuses on improving the efficiency of heat engines by recovering low-grade waste heat using an aqueous-based thermoelectrochemical cell.

More than 90% of the energy we use comes from thermal process, which produces the bulk of the electricity generated by power plants, as well as powering airplanes and most cars. Heat engines have existed since the Industrial Revolution and gave rise to the science of thermodynamics. However, heat engines, as a popular energy generation process, are typically only 30% to 55% efficient, and abandon roughly 15 terawatts energy in the form of waste heat to the environment. In fact, there is almost 60% of total energy generated in United States are counted as rejected energy in a year as show in Figure 1 [2].

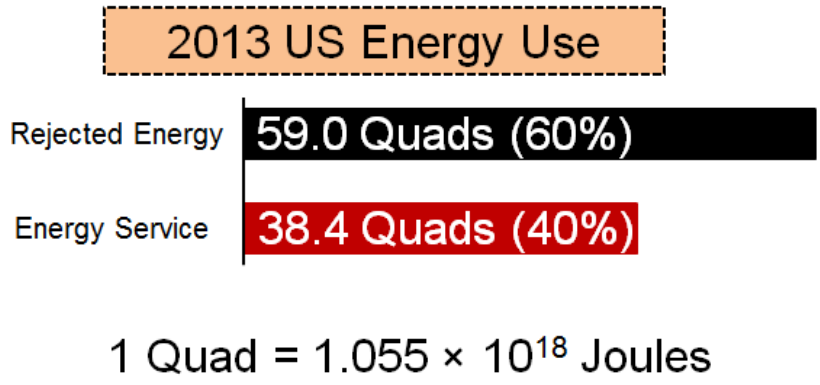

Figure 1: Estimated United States energy use in 2013

One typical example of heat engines' energy loss is internal combustion engines (ICEs). Typical energy split of an ICE is shown in Figure 2, in which only 21.5% energy generated from it is used as effective power to move the car. Waste heat constitutes 30-37% of the energy as a result of exhaust gas with lower

energy content and convection. Other losses in an ICE include mechanical losses (33-40%), air drag (3-12%), rolling friction (12-45%) and brake losses (about 5%) [1].

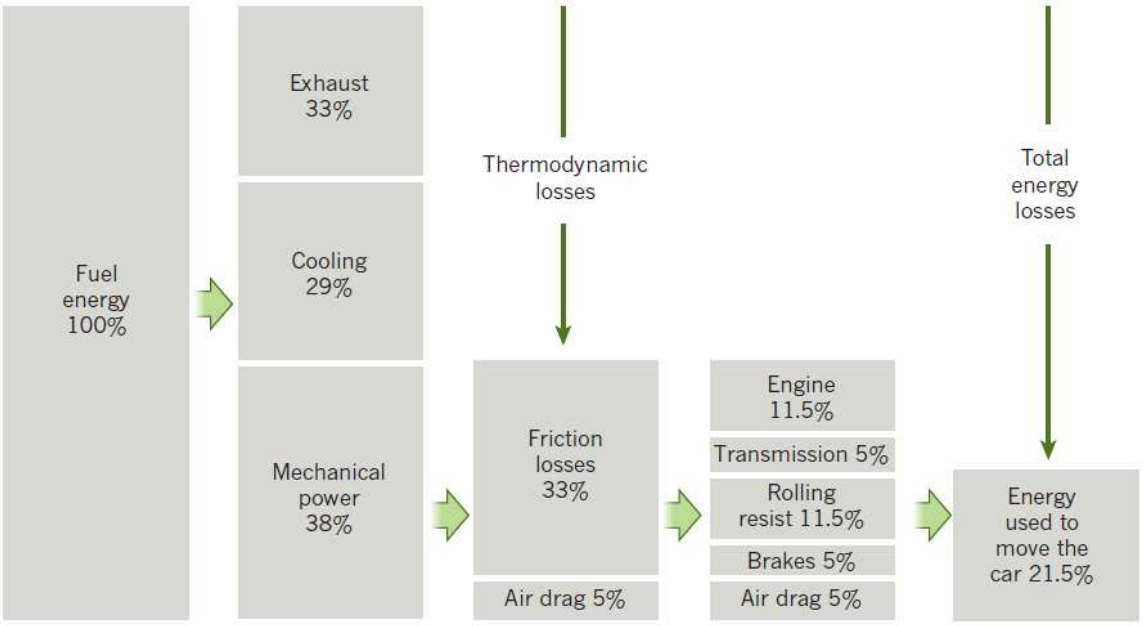

Figure 2: Vehicle energy losses

The above information concludes that there exist great opportunities for improving heat energy efficiency by converting waste heat into useful energy and electricity. In general, organic Rankine Cycle (ORC) as a thermodynamic cycle that essentially converts heat into mechanical work, provides a method for recovering large-scale waste heat recovery in power plant or heavy-duty vehicles. ORC also can be used to generate energy from solar, biomass and geothermal [6]. Thermoelectric materials and generators provide an efficient to convert low-grade waste heat into useful electricity according to Seebeck effect and thus improve overall efficiency of heat engines.

1.2 Thermoelectric Effect

1.2.1 Seebeck Effect

The Seebeck effect was discovered by the German physicist Thomas Johann Seebeck in 1821. It describes the phenomenon in which a circuit formed from two or more different conductors produces an electromotive force (emf) in a temperature gradient and consequently an electric current. Figure 3 provides a reference which can conveniently explain this effect in details: two dissimilar conductors, a and b (referred to in thermoelectrics as thermocouple legs, arms, thermoelements, or simply elements and

sometimes as pellets by device manufacturers) which are connected electrically in series but thermally in parallel [7]. If the junctions at A and B are maintained at different temperatures T_{hot} and T_{cold} and $T_{hot} > T_{cold}$, an open circuit emf and a voltage gradient ΔV is developed between C and D which is given by [7]

$$\Delta V = \alpha(T_{hot} - T_{cold}) \; or \; \alpha = V/\Delta T$$

which defines the differential Seebeck coefficient α between the elements a and b in $\mu V/K$. In general, the relationship is linear in a small temperature gradient, and Seebeck coefficient can be also referred as the thermal emf or thermopower. In this research project, the maximum temperature difference is 45 Kelvins, and the Seebeck coefficient presents linear relationship of voltage gradient and temperature gradient.

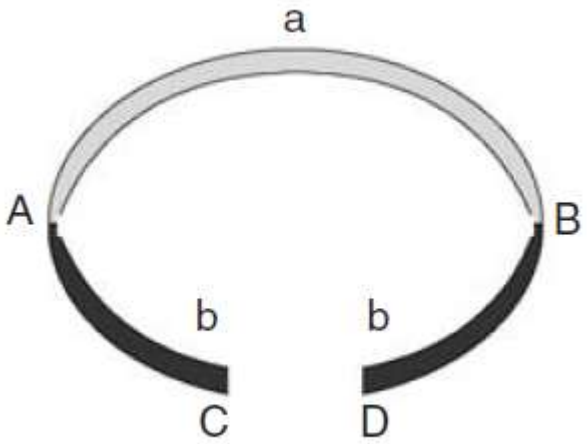

Figure 3: Schematic basic thermocouple

Solid state physics provides a more theoretical insight on Seebeck effect: compare to the colder side, the warmer side of a conductor has more thermal energy in the form of higher average electron momentum. Therefore, these free electrons on the warmer side migrate faster towards the colder side compare to these free electrons on the colder side migrate towards warmer part which leads to a more negative charge at colder part than warmer part and it can cause a generation of emf and consequently an electric current.

1.2.2 Figure of Merit (ZT)

According to the second law of thermodynamic, in order for heat engines to deliver works, heat engines have to operate between a heat sink at a colder temperature (T_{cold}) and a source of heat at a warmer temperature (T_{hot}), and the maximum efficiency can be achieved by a heat engines in the temperature gradient (ΔT) is defined as Carnot efficiency (η_{max}) [8]:

$$\eta_{max} = 1 - \frac{T_{cold}}{T_{hot}}$$

Thermoelectric (TE) modules using Seebeck effect which enable direct conversion between waste heat and useful electricity, and provide an alternative approach for power generation for waste heat recovery. The fraction of the Carnot efficiency of a thermoelectric cycle is quantified by the thermoelectric figure of merit ZT of the system as a whole, which is the average ZT of the n- and p-type semiconductor s, where:

$$ZT = \frac{\sigma \alpha^2 T}{\lambda}$$

which depends on thermal conductivity λ, Seeback coefficient α, electrical conductivity σ and temperature T [23]. To have a high efficiency for a typical thermoelectric material, its value of ZT need to be higher which means a semiconductor at a specific temperature gradients with superior electrical conductivity and lower thermal conductivity will be more efficient for converting waste heat to useful electricity. The goal of thermoelectric research focus on seeking new materials which could achieve maximum ZT, by maximizing the value of $\sigma\alpha^2$ and minimizing λ.

The maximum efficiency of a thermoelectric material depends on the Carnot efficiency, for all heat engines cannot exceed Carnot efficiency, and thermoelectric properties as mentioned in previous paragraph, like Seebeck coefficient, electrical conductivity and thermal conductivity. For large temperature difference this efficiency is given by [24]:

$$\eta_{max} = \frac{T_{Hot} - T_{Cold}}{T_{Hot}} \frac{\sqrt{1+ZT} - 1}{\sqrt{1-ZT} + \frac{T_{Cold}}{T_{Hot}}}$$

1.2.3 Electrical Conductivity

Electrical conductivity σ is used to specify the electrical character of a material which is simply the reciprocal of the resistivity, or

$$\sigma = \frac{1}{\rho}$$

and is indicative of the ease with which a material is capable of conducting an electric current.

A material's electrons seek to minimize the total energy in the material by going to lowest energy states in an atom. According to the Pauli Exclusion Principle, there are maximum two electrons with opposite spins can reside in the same orbital. The electrons occupy the energy states from the lowest value, and then level up to which the electrons have filled is called the Fermi level. The position of the Fermi Level with respect to the band structure is very important for electrical conduction in metals and semiconductors: only electrons in energy levels near the Fermi level are free to move around.

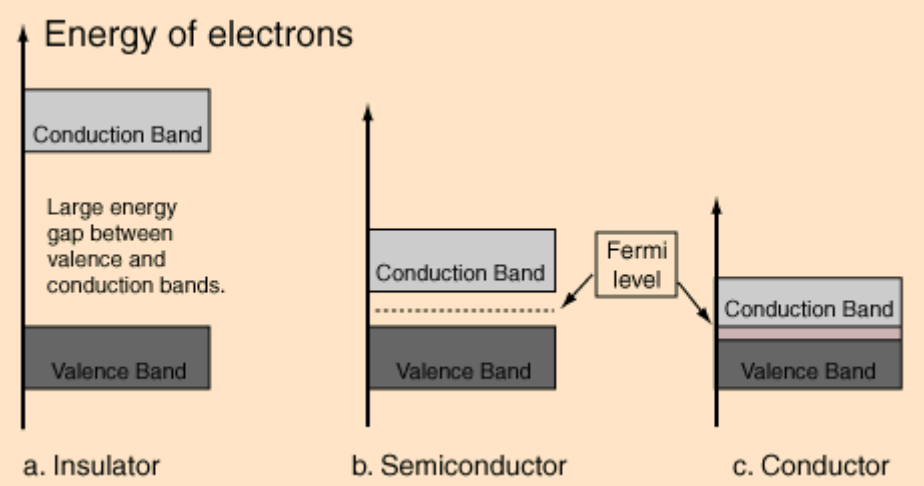

Figure 4: Explanation of metals, insulators, and semiconductors based on the one-dimensional band structure

As shown in figure 1-4 (c), in metals, the Fermi level lies in the conduction band giving rise to free conduction electrons which means there are many electrons available to move in metals. Therefore, metals present high electrical conductivity. However, in semiconductors the position of the Fermi level is within the band gap, approximately half-way between the conduction band minimum and valence band maximum for undoped semiconductors (Figure 4 (b)). In doped semiconductors, dopant atoms increase the majority charge carrier concentration by donating electrons to the conduction band or accepting holes in the valence band. In electrolytes, electrical conduction is caused by ions movement in solution as each carrying an electrical charge [9].

1.2.4 Thermal Conductivity

Thermal conduction is the phenomenon by which heat is transported from high- to low-temperature regions of a substance. The property that characterizes the ability of a material to transfer heat is the thermal conductivity. It is best defined in terms of expression:

$$q = -\lambda \frac{dT}{dx}$$

where q denotes the heat flux, or heat flow, per unit time per unit area (W/m^2), λ is the thermal conductivity which has unit as W/m-K, and *dT/dx* is the temperature gradient through the conducting medium [10].

1.2.5 Thermoelectric Modules

As mentioned in 1.2.3, impurities (more commonly called dopants) may have an energy level

close to that of the conduction band. Electrons can be excited from the impurities and fall into the conduction band, resulting in more electrons than holes. Such a semiconductor is called an n-type semiconductor and the dopants are called donors. When the impurity energy levels are close to the valence band, electrons are excited from the valence band into the impurity level, leaving more holes behind. Such semiconductors are called p-type and the impurities are called acceptors [11].

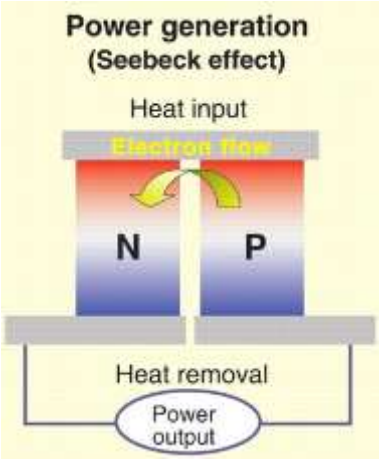

Figure 5: Practical thermoelectric generators connect large numbers of junctions in series to increase operating voltage and spread heat flow [3].

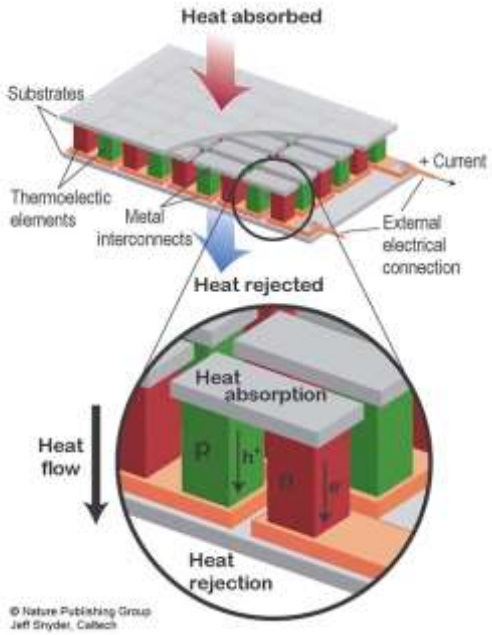

Figure 6: A thermoelectric module is an array of thermocouples connected electrically in series but thermally in parallel. [24]

The construction of thermoelectric modules consist of pairs of n-type and p-type semiconductor materials as a thermocouple with one side connected to a heat source and another side to a heat sink (Figure 5). These two types semiconductor are arranged in an array in which they are connected electrically in series and thermally in parallel. (Figure 6) In the temperature gradient, electrons and holes tend to accumulate on the cold side. An electric field *E* develops between the cold side and the hot side of each material, which gives a voltage when integrated over the length of each thermoelements. The voltages of the n- and p- type semiconductors add up and drive an electrical current through an electrical load, here an electrical resistor. The product of the voltage and the current is the electrical power output of the generator. Therefore, once there is a temperature gradient exists between two sides of thermoelectric modules, those thermocouples can be used to generate electricity.

1.3 Brief Efficiency Review in Solid-State Thermoelectrical Materials

There is no theoretical upper limit to ZT, and no known materials have a ZT greater than 3 to date. In 2003, a team from Michigan State University led by Kanatzidis invented a complex bulk tertiary material which has a ZT of at least 1.4 at 780 K [25]. In 2008, Professor J.P. Heremans at Ohio State University announced that they had reached a ZT of 1.5 at 780 K [26]. A research team consists of material scientists and mechanical engineers from Northwestern University and Michigan State University claim that they developed a new thermoelectric material which has a thermoelectric figure of merit of 2.2 at 915 K, which is the highest by 2012. By having this figure of merit at 915 K and a figure of merit equals to 1.2 at 350 K, it could have a predicted that thermoelectric generators could have waste heat conversion efficiencies of 16.5% to 20% with a cold-side temperature of 350K and a hot-side temperature of 950K. [4] This led to possible broad-based applications in automotive waste heat recovery and has 8% fuel economy improvement with 40% heat loss in exhaust gas.

1.4 Motivation

Classical solid-state thermoelectric materials potentially provide an approach to improve the efficiency of heat engines by converting waste heat directly into useful electricity, but have limited application due to their low energy conversion efficiency and low-abundance elements that post challenges for scale-up, as they entail high material costs [12].

This research project intends to seek for lower cost thermoelectric materials with high energy conversion efficiency as conventional power cycles. The project mainly focuses on investigating the theoretical study on thermoelectric effect in electrolytes as a function of temperature gradients and proton concentration gradients. It also has an experimental study part which tests the thermopower of electrolytes and experimentally proves our new principle and establishes a new fundamental theory: In the presence of

a concentration gradient (internal voltages), if an electrolytes in which cations have larger ions mobility and charges than anion, then the system should be able to generate electricity from heat. This new principle could be later applied to low-grade waste heat recovery for variant applications.

1.5 Overview of Thesis

This thesis consists of four chapters in total. Chapter one provides a brief introduction and review of thermoelectric effect, solid-state thermoelectric materials and national energy security. Chapter two focuses on the introduction of a new principle which can be used to harvest waste heat using electrolytes. Chapter three is the experimental study part which provides experimental results of a thermoelectrochemical cell, including pH measurement, electric conductivity, power output and ZT. Chapter four discusses conclusion of this research project and potential future work, and the key contributions of this thesis.

Chapter 2: Theoretical Study

(Part of Chapter 2 and Chapter 4 contents were copied from Professor Anne Co and Professor Joseph Heremans's NSF proposal on Thermoelectrochemical Generator with Permission)

2.1 Literature Review

The fundamental theory in this research project is that thermoelectrochemical effects can occur in electrochemical cells which subjected to a temperature difference and can be used to generate useful electrical power. The mechanisms that give rise to an electrical voltage fall in several main categories (Figure 7). The nomenclature used in this thesis is somewhat confusing, a short review of past work will be presented first, in order to better differentiate the idea behind the basis of this research project.

The first category (Figure 7a) encompasses electrochemical cells that are charged at a high temperature, and then discharged at a lower temperature. From an electrochemical point of view, they can be viewed as batteries that are charged by heat instead of a charging current. From a thermal point of view, they can be described by a classical thermodynamic cycle in a (temperature, entropy) diagram [13,14].

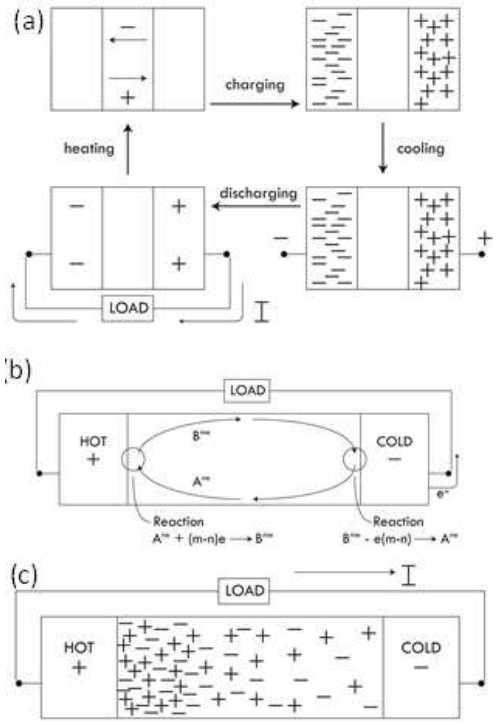

Figure 7: Different types of thermoelectrical cells

The second category are thermogalvanic cells [16] as shown in Figure 7b. These are electrolytic cells that have two electrodes of the same composition and separated by an electrolyte. A temperature

difference exists between the two electrodes. The basic idea is that a chemical redox reaction takes place at the hot electrode and another one at the cold electrode, with the products of the reaction formed at one of the two electrodes becoming the reactants of the reaction at the other electrode, similar to a redox flow cell. These two reactions must involve the emission of a charge at one of the two electrodes and its absorption at the other generating a voltage across the cell. In this type of cell the charge transport is accompanied by a mass-transport process, required to transfer the reaction products and reactants between the hot and the cold electrodes. The underlying transport phenomenon is thermophoresis (also known as the Soret effect) of electrically charged particles. Thermophoresis is a phenomenon observed in mixtures of mobile particles where the different particle types exhibit different responses to the force of a temperature gradient. The mass transport can be enhanced by convection.

2.2 New Concept and Theory of Operation

2.2.1 Thermopower of Each Ion in Aqueous Solution

In this research project, a different and a new category is proposed, as shown in Figure 7c, based on ambipolar thermoelectric transport. In this configuration, at each point x in the electrolyte along the length of the cell, the concentration of anions (n_-) and cations (n_+) is the same ($n_+(x) = n_-(x)$). At each point x there is charge neutrality in the electrolyte. The electrolyte is chosen so that these concentrations are very temperature-dependent, i.e. so that

$$\frac{\partial n_-}{\partial T} = \frac{\partial n_+}{\partial T}$$

is large. This then implies that a gradient in temperature $\nabla_x T$ in the cell generates a spatial gradient in concentration,

$$\nabla_x n_+ = \nabla_x n_- = \left(\frac{\partial n_-(x)}{\partial T}\right)_x \nabla_x T$$

even when local thermodynamic equilibrium is achieved and charge neutrality is maintained at each point x. This concentration gradient in the purely static picture would therefore not create a potential difference between hot and cold electrodes. But transport properties are not at thermodynamic equilibrium: the presence of the gradient $\nabla_x T$ implies, by the Onsager relations, a small departure from equilibrium when the whole cell is considered, even if each infinitesimal section at x is at local equilibrium.

Consider now the case of only the positively charged carriers (which in aqueous solutions would be cations, but could really be any charged mobile objects, such as vacancies or interstitials in a solid for example) in Figure 7c: there is a gradient in concentration $\nabla_+ n_+$ Considered in isolation (i.e. ignoring the presence of negatively charged particles), the presence of $\nabla_+ n_+$ at a point in local thermal equilibrium at

temperature T(x) implies the presence of a gradient in local electrochemical potential $\nabla_+\mu_+$ and thus of a local electric field:

$$E_+(x) = -\nabla_x\mu_+$$

Since it is the presence of $\nabla_x T$ that drives all this, there is therefore a local partial thermoelectric power:

$$\alpha_+ \equiv \frac{E_+(x)}{\nabla_x T}$$

Continuing the assumption that the transport properties are linear (i.e. the fluxes proportional to the gradients), the properties of the complete cell can be integrated over the cell length, over which a partial hole thermoelectric voltage V_+ appears in the presence of the temperature difference

$$\Delta T = T_{hot} - T_{cold}$$

between the electrodes (assumed to be at thermal equilibrium with the electrolyte directly in contact with them). One can then also define a device thermopower:

$$\frac{V_+}{\Delta T} = \frac{\int_{cold}^{hot} E_x(x)dx}{\int_{cold}^{hot} \nabla_x T dx}$$

The exact same reasoning can be held concerning the negatively charged particles (anions) considered in isolation, and a partial thermopower can be defined for them as well:

$$\alpha_- \equiv \frac{E_-(x)}{\nabla_x T}$$

The sign of the partial thermopower is that of the charge: $\alpha+ > 0$ and $\alpha- < 0$.

2.2.2 Ambipolar Ions Transport

Ambipolar conduction arises from solving the transport properties of the two types of charged particles, not in isolation, but together. If the properties of the positively and negatively charged particles were identical, one would have a zero net effect, but those properties are never identical. Instead, if the cations and anions are chosen to have very different transport properties, a substantial thermoelectric voltage can be made to develop: this is the premise for the ambipolar cell that we propose to develop here. To create an estimate of the ambipolar thermoelectric power, one must solve the transport equations for the positive and negative ions together. This is done, by analogy with the case of solids [17] by solving three sets of equations for each infinitesimal section of electrolyte.

1. The local equilibrium condition dictates that the electrochemical potential μ for the whole system is equal for both positively and negatively charged particles:

$$\mu = \mu_+ = \mu_-$$

2. The total flux of electrical current is the sum of the contributions from both positively charged and negatively charged species:

$$j = j_+ + j_-$$

3. The total flux of heat is the sum of the contributions from both types of particles:

$$j_q = j_{q+} + j_{q-}$$

Note that when no current is drawn from the system, j = 0, but, in the presence of a temperature gradient, the partial j+ and j – are not necessarily both zero, as they can be equal and of opposite polarity. The heat fluxes are also not zero. These equations are substituted in the Onsager transport equations, and the solutions expressed in terms of partial cation and anion conductivities:

$$\sigma_+ = n_+(z_+e)u_+;$$
$$\sigma_- = n_-(z_-e)u_-$$

(see equivalent electrical circuit in Figure 8).

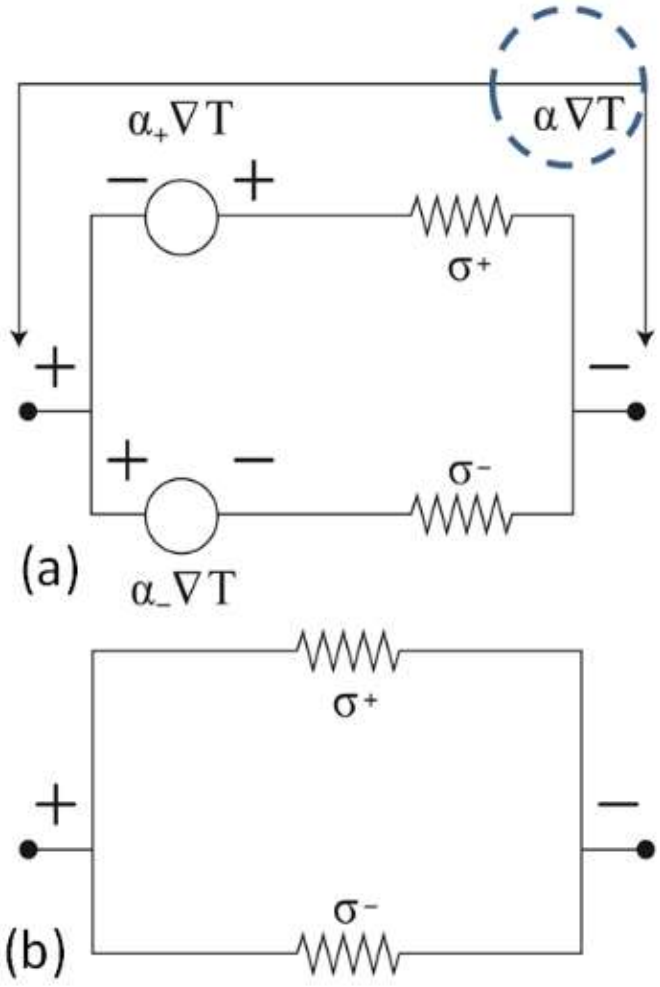

Figure 8: Equivalent circuit for ambipolar transport

In these equations, $z_{+,-}$ denote the ionization state of each oions, and u_+, u_- the cation and anion mobilities, respectively. The total ionic conductivity of the electrolyte is then the ambipolar conductivity:

$$\sigma = \sigma_+ + \sigma_- = n_- e(z_+ u_+ + z_- u_-) \quad (1)$$

and the total thermopower is also the ambipolar thermopower given by:

$$\alpha = \frac{\alpha_+ \sigma_+ + \alpha_- \sigma_-}{\sigma} = \frac{\alpha_+ z_+ u_+ + \alpha_- z_- u_-}{z_+ u_+ + z_- u_-} \quad (2)$$

Equation (2) can be expressed in terms of the effective mobility ratio:

$$\beta \equiv \frac{z_- u_-}{z_+ u_+}$$

Where

$$\alpha = \frac{\alpha_+ + \alpha_- \beta}{1 + \beta} \quad (3)$$

If anions and cations have symmetrical properties, except that one has a negative and the other a positive partial thermopower,

$$\beta = 1, \alpha_- = -\alpha_+, and\ \alpha = 0$$

as expected. However, if we further assume that the mobility of the positively charged ion (e.g. H_+) is much higher than that of the negatively charged ion (e.g. NO_{3-}),

$$u_+ \gg u_-, \beta \ll 1\ and:$$

$$\alpha \approx \alpha_+ \quad (4)$$

The result for ambipolar transport in Eq. (2), and its limit in Eq. (4), can be understood intuitively by considering cations and anions in and electrolyte subject to a temperature gradient as two independent voltage sources (Figure 8). The equivalent circuit for an infinitesimal slice of the electrolyte at position x of the cell Figure 7c in the presence of a temperature gradient is given in Figure 8a, where the anion and the cation channel work like two voltage sources connected in parallel. Each voltage source gives a voltage:

$$V_{+,-} = \alpha_{+,-} \nabla T$$

and each has an internal source resistance which the inverse of its conductance $\sigma_{+,-}$. The circuit gives an electric field in that slice that is:

$$E = \alpha \nabla T$$

with the net ambipolar thermopower α given by Eq. (2). The ambipolar electrical conductivity, Eq. (1), is illustrated by the circuit in Figure 8b. Figure 8 also serves the purpose of illustrating that a net non-zero current circulates between the anion and cation channels, even if there is no net current leaving the infinitesimal slice of electrolyte.

2.2.3 Advantages of Electrolytes as Thermoelectric Materials

The ambipolar thermoelectrochemical cell that now behaves like a classical solid-state thermoelectric material, except that it would also work in a liquid, amorphous, and solid electrolytes. This has the following advantages and disadvantages when compared to classical thermoelectrics.

1. The electrolyte has a much lower thermal conductivity (λ) than almost all classical thermoelectrics. Water has λ =0.7 W/m-K, considerably less than commercial thermoelectric materials (PbTe and Bi_2Te_3-based materials have $\lambda \sim 2$ W/m-K). This is an inherent advantage of a solution-based or amorphous electrolyte.
2. In a solution based system, we can take advantage of the flexibility and richness of solution based chemistry of ionic conductors for tuning the voltage dependence over a thermal gradient.
3. In aqueous solutions, proton mobility is generally much higher than the mobility of any anion, which translates to the thermoelectric voltage measured to be predominantly dependent on the proton concentration, as $\beta << 1$. This hypothesis will be examined by exploring the dependence of acid/base equilibrium with temperature, using acids, bases and buffers.

2.2.4 Theoretical Thermopower Equation

To complete this section, a new theory is developed for the partial thermopowers $\alpha_{+/-}$ of the particles in Figure 7c, at least in solution. Considering the ions in solution as an ideal gas, and use the kinetic gas theory. The thermopower of an ideal gas is the entropy per particle [17]:

$$\alpha = \frac{S}{ne} = \frac{C_v}{ne},$$

where *S* is the entropy and C_V specific heat per constant volume of the whole system.

$$C_v = \frac{dU}{dT}$$

with *U* the internal energy given by [19]

$$U = nk_BT$$

where k_B is the Boltzmann constant. This internal energy depends on temperature not only via the explicit factor T, but also via the formation/annihilation of the particles themselves, since their concentration is strongly T-dependent. Therefore

$$C_V = k_B\left(n + \frac{Tdn}{dT}\right)$$

The partial thermopower becomes:

$$\alpha = \frac{k_B}{ne}\left(\frac{Tdn}{dT} + n\right) = \frac{k_B}{e}\left(1 + \frac{dln(n)}{dln(T)}\right) \quad (5)$$

In the case where the proton is the cation, and Eq. (5) can be expressed in terms of *pH*, by writing:

$$\ln(n) = \ln(M \times A \times 10^3) = 2.3\log(M) + \ln(10^3 A) = 2.3pH + \ln(10^3 A),$$

where M is the molarity of the solution, A is Avogadro's number, and the concentration n is molecules per cubic centimeters, or 0.001 liter. Substituting this into Eq. (5) yields:

$$\alpha_{H_+} = \frac{k_B}{e}\left(1 + \frac{2.3TdpH}{dT}\right) \tag{6}$$

2.3 Experimental Procedures

2.3.1 Theoretical Analysis - pH

According to the new theory, a concentration gradient can be created under temperature gradient in an electrolyte. To prove the concept, barium nitrate ($Ba(NO_3)_2$ and 15 M nitric acid (HNO_3) electrolyte system was selected in this research project. The reason for selecting ($Ba(NO_3)_2$ and (HNO_3) is due to the fact that ($Ba(NO_3)_2$ has a large solubility variation in the temperature from 20 ℃ to 100℃, and thus it can create large proton concentration gradient in the electrolytes. Also the ions involved in the transport have a room temperature mobility of:

Table 1: Ions mobility

Ions	Mobility
H^+	36.30×10^{-4}
NO_3^-	7.40×10^{-4}
Ba^{++}	6.59×10^{-4}

so that the condition $\beta << 1$ is met for proton transport.

Here, the concentration gradient is built upon the temperature-dependent solubility of $Ba(NO_3)_2$ in water. We rely on the temperature dependence of the chemical equilibrium, where K_a is the acid dissociation constant and K_{sp} is the solubility constant. Acid dissociation constants of common acids are generally less temperature dependent than the dissociation (or solubility) constant of insoluble salts. We therefore introduced a series of chemical equilibria where the temperature dependence of $Ba(NO_3)_2$ dissociation influences the proton concentration in solution in the presence of nitric acid, represented in the following equations:

$$Ba(NO_3)_2 \overset{K_{sp}}{\Leftrightarrow} Ba^{2+} + 2NO_3^-$$
$$HNO_3 \overset{K_a}{\Leftrightarrow} H^+ + NO_3^- \quad (7)$$

Thus, the equilibrium constant can be written as followings:

$$K_a = [H^+][NO_3^-]$$

and [HNO_3] is ignored due to the fact of strong disassociation ability of Nitric Acid.
and:

$$K_{sp} = [Ba^{2+}][NO_3^-]^2$$

and [$Ba(NO_3)_2$] is ignored because it is in solid form at the measuring temperatures. The proton concentration then can be obtained:

$$[H^+] \approx Ka\sqrt{\frac{[Ba^{2+}]}{Ksp}} \quad (8)$$

as a function of temperature.

By the definition of pH:

$$pH = -\log_{10}[H^+] = \log_{10}\frac{1}{[H^+]}$$

which is the decimal logarithm of the reciprocal of the hydrogen ion activity, [H^+], in a solution [20].

A theoretical calculation of pH was then performed based on the above equations with the information of K_a and K_{sp} from the Handbook of Chemistry and Physics. The theoretical results are shown in Figure 9. Based on the results show in Figure 9, there is a slight pH or proton concentration decreases as there are more barium nitrate or nitrate ion dissolved into water with increasing temperature. Therefore, a concentration gradient can be generated in the thermoelectrochemical cell in a temperature gradient.

2.3.2 Theoretical Analysis – Thermopower

The theoretical value of pH then can be substituted into Equation (5) to calculate the theoretical thermopower of barium nitrate system. Table 2 lists the values for calculating theoretical thermopower. Based on the values in Table 2:

$$\alpha_{H_+} = \frac{k_B}{e}\left(1 + \frac{2.3TdpH}{dT}\right) = -498\ \mu V/K$$

This is the average value in the temperature range from 295.5 K to 335.5 K which is the range the experiments were performed, and the isothermal temperature in this research project was 315.5 K which is used to calculate the ZT of the barium nitrate system.

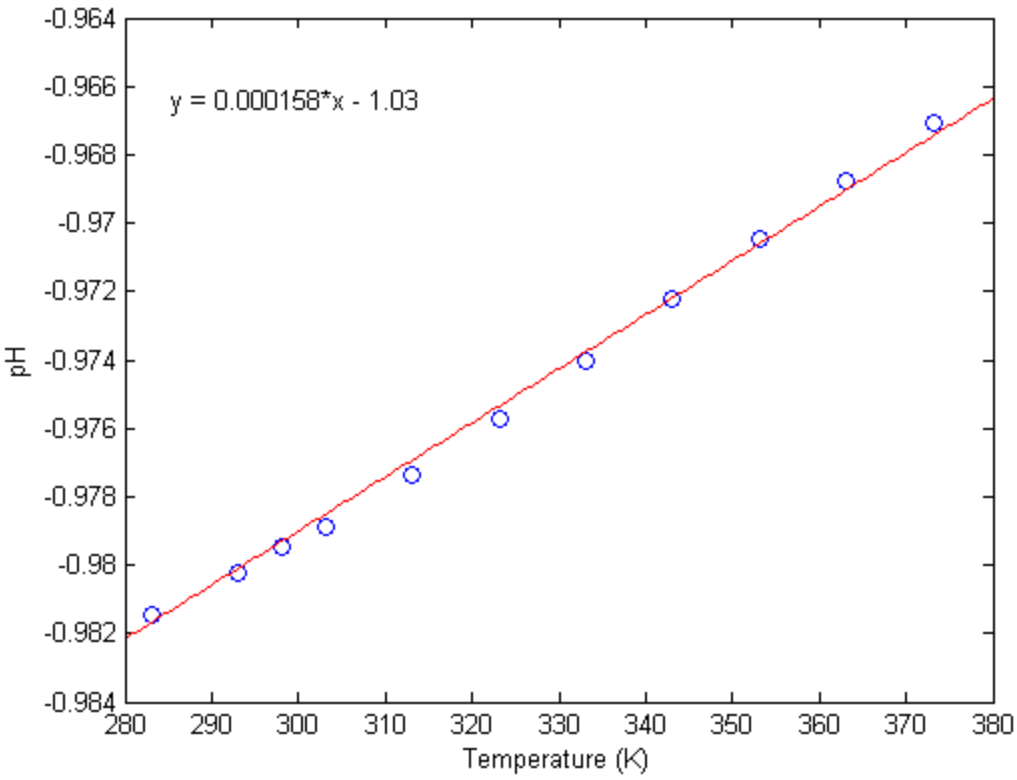

Figure 9: Theoretical pH Barium Nitrate system as a function of temperature

Table 2: Data for Calculating Theoretical Thermopower

ln(T) [K]	T[°C]	$[NO_3^-]$ [moles/L]	$1/[NO_3^-] = [H^+]_{a.b.s.}$	$\ln[H^+]$
5.609	0	0.377	2.653	0.975
5.645	10	0.514	1.961	0.673
5.680	20	0.682	1.610	0.480
5.697	25	0.782	1.280	0.250
5.714	30	0.865	1.154	0.140
5.746	40	1.075	0.930	-0.070
5.778	50	1.303	0.767	-0.265
5.808	60	1.541	0.649	-0.432
5.838	70	1.790	0.559	-0.582

Chapter 3: Experimental Study

3.1 Hardware Design

The thermoelectrochemical cell consists of two glass reaction cells which connect with each other through a glass channel with a uniform diameter of 1.5 centimeters (Figure 10). The length of the channel is about 10 centimeters. On top of each reaction cells, two holes allow non-reacting platinum (Pt) electrodes and thermometers being immersed in the electrolytes ($Ba(NO_3)_2$ and HNO_3). The holes were then sealed using O-rings which were attached to both electrodes and thermometer. The thermometers were used in this research project to measure the temperature of each reaction cell, and two electrodes were connected to an electrochemical analyzer (Potentiostats) to measure the open circuit voltage output from the thermoelectrochemical cell.

In addition, glass wool was inserted into the connecting channel which acted like a heat insulator to prevent heat convection from hot reaction cell to cold one, but still allowed ions move from one reaction cell to another.

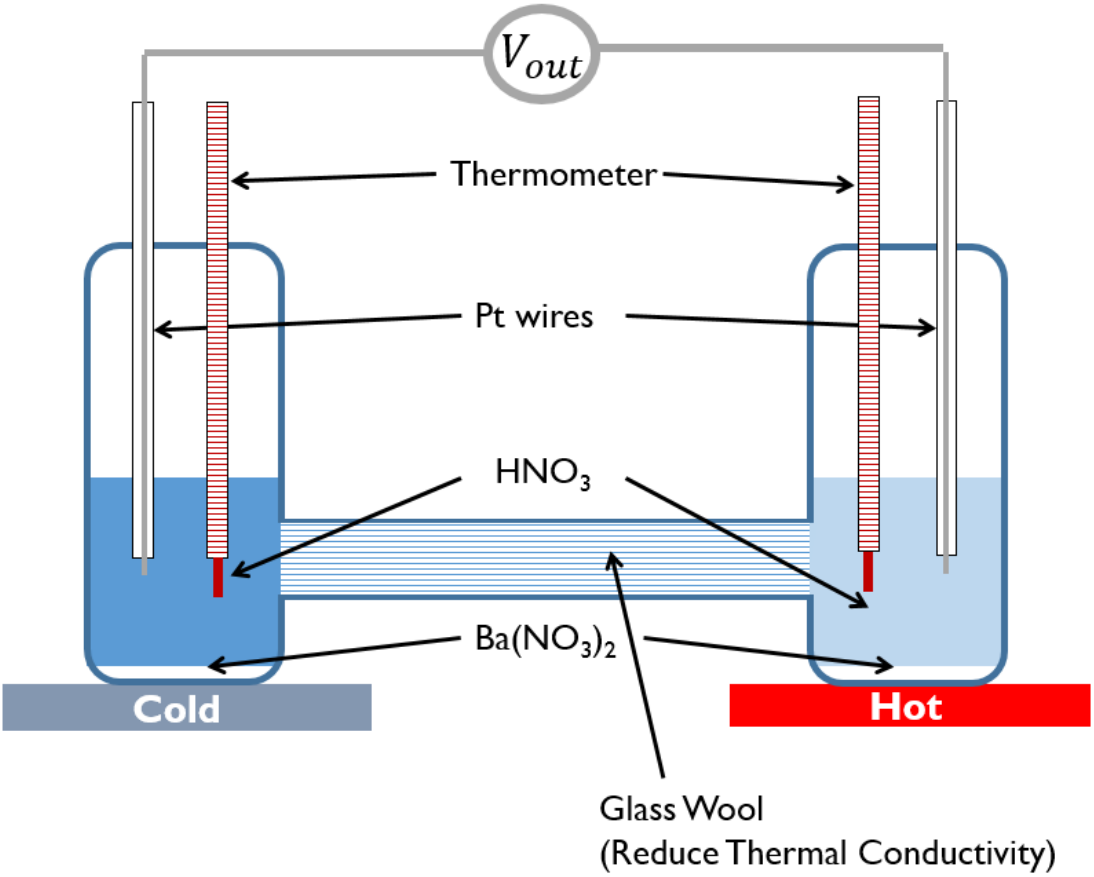

Figure 10: Experimental Schematic

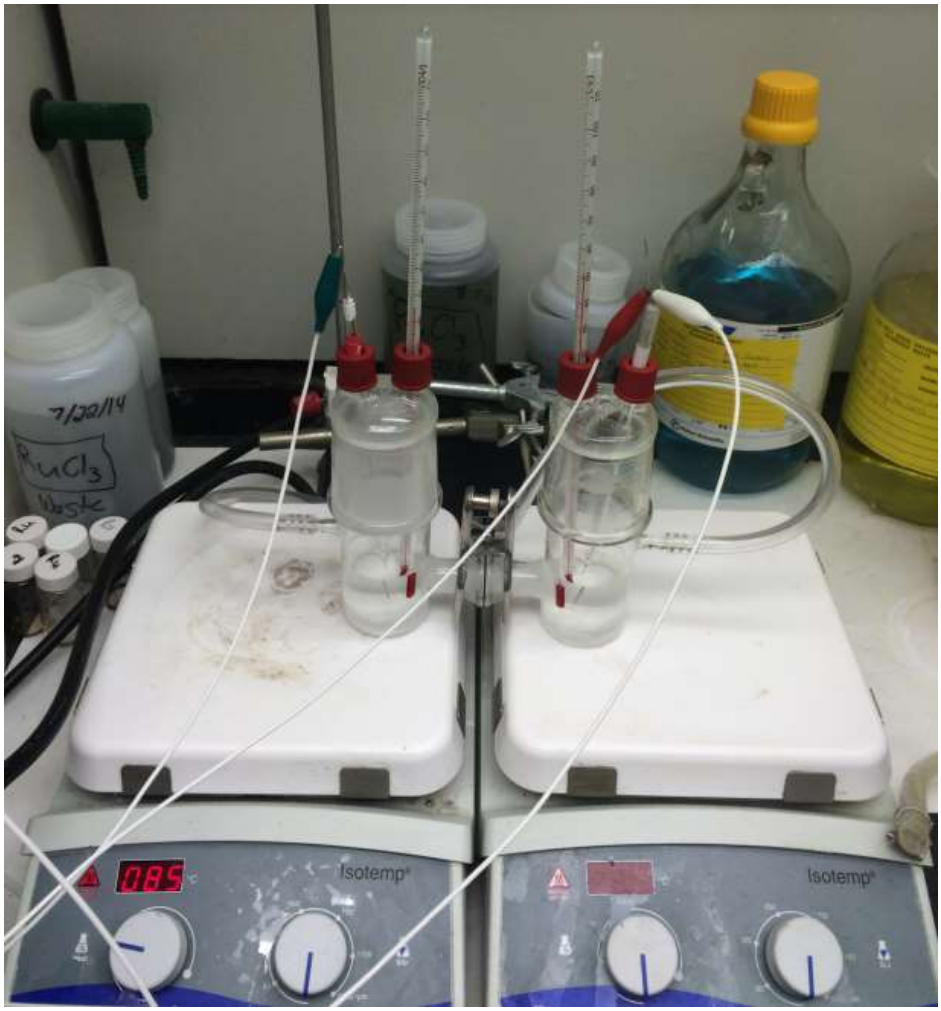

Figure 11: Experiment Set Up

The bottom of each reaction cells was set on two separate hot plate (Figure 11). The left side reaction cell was treated as a cold one or heat sink, and the right side was a hot one or heat source. Each reaction cell also has an orifice which was connected to each other using a plastic tube to prevent any HNO_3 or NO_2 gas leakage from the thermoelectrochemical cell.

The total volume of each reaction cells is about 300 ml, and each of them was not entirely filled with electrolytes. Interface reaction between electrolytes and air inside the reaction cell was not considered in this research project as it only had small affect to the overall reaction. The temperature distribution in each reaction cell was assumed to be uniform.

3.2 Experiment Preparation

3.2.1 Thermopower Measurement Preparation

The Platinum electrodes were all cleaned using piranha solution (a mixture of sulfuric acid (H_2SO_4) and hydrogen peroxide (H_2O_2)) before each measurement to remove any organic residues from electrodes, and ensure the accuracy of measurement.

The operating temperature of this experiment was from 293 K to 343 K (20 ℃ to 70 ℃) to ensure the safety of research experiment as the boiling point of nitric acid is 356 K (83℃).

In this research project, 120 ml 15 M nitric acid (HNO_3) and 20 grams barium nitrate ($Ba(NO_3)_2$) were used to measure the thermopower of the mixing electrolyte of HNO_3 and $Ba(NO_3)_2$. Excess amount of $Ba(NO_3)_2$ ensured the saturation of $Ba(NO_3)_2$ in the electrolyte throughout experimental operating temperature range, and thus created a proton concentration gradient in the electrolytes.

3.2.2 Electrical Conductivity and pH Measurement Preparation

300 ml 15M nitric acid and 30 grams barium nitrate were used to measure the electrical conductivity and pH of the electrolyte. Electrical conductivity meter was used as the instrument for measuring electric conductivity of the electrolyte, and it was measured under a temperature increment of 10 K. Electrical conductivity meter was calibrated using 0.1 M KCl and 0.01 M KCl at room temperature before each measurement, and the electrical conductivity of 0.1 M KCl and 0.01 M KCl are available at online sources [21].

The method used for measuring pH was titration. The original method was using a pH meter, however, multiple ions presented in the electrolyte which could potentially affect the accuracy of the pH meter measurement. Therefore, a more traditional pH measurement method – titration, was adopted in this research project. The base used in titration is 6M NaOH. The volume of electrolyte for each titration was 10 ml. Bromthymol blue was used as pH indicator which change color at pH = 7.6 from yellow to blue.

3.3 Experiment Results

3.3.1 Thermopower Measurement

To measure the thermopower of the electrolyte or thermoelectrochemical cell, the hot side reaction cell was first heated up to 62.5 ℃ (335.5 K) and the cold side was first maintained at room temperature which was 22.5 ℃ (295.5 K). Then the hot side temperature was gradually decreased to 42.5 ℃ (315.5 K) by an increment of 5 K, and the cold side temperature was gradually increased to 42.5 ℃ (315.5 K) by an increment of 5 K (Figure 12). Therefore, the average temperature of the thermoelectrochemical cell was maintained at 42.5 ℃ (315.5 K). For an increment of 5 K, there was a

measurement point.

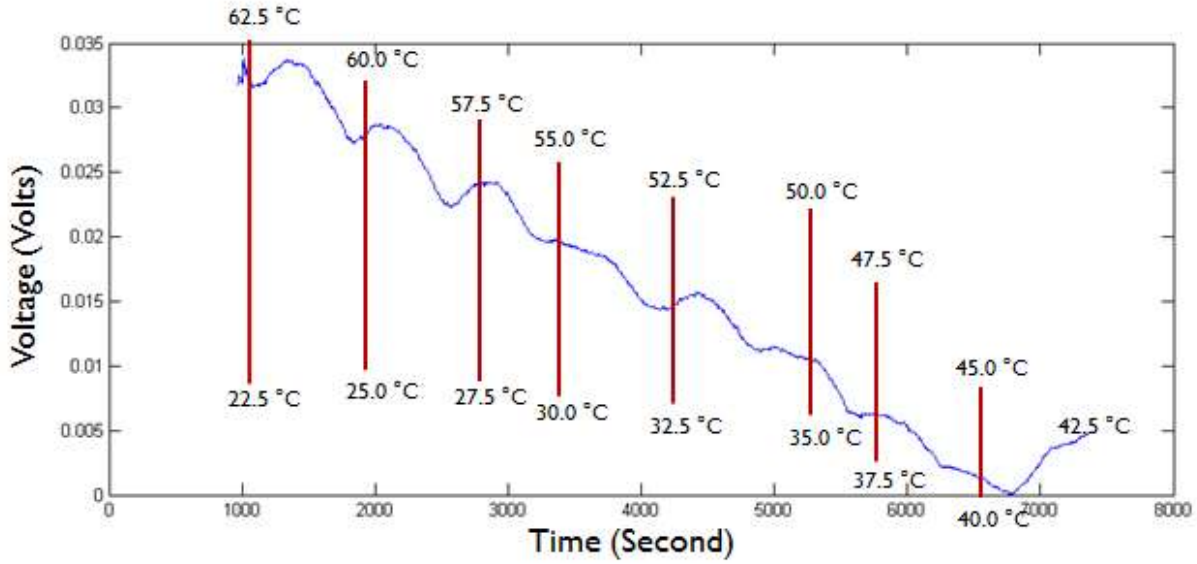

Figure 12: Absolute Raw Data Value for Thermopower (Seebeck Coefficient) Measurement

As it shows in Figure 12, the open circuit voltage output decreases with decreasing temperature gradient which proves our new principle and the Seebeck effect in electrolytes.

For each measurement points, the temperature was kept constant or isothermal, and there was very small temperature drift during the measuring. Also, 60 seconds measurement or over 1000 data were collected at each measurement points. The average values of open circuit voltage output of each measurement points were taken to minimize the measurement error. Figure 13 and Table 3 relates those average voltage output values with corresponding temperature gradient, and it shows a linear relationship of output voltage with temperature gradient. Take the slope of the thermopower data in Figure 13, and the measured thermopower is about 901.5 $\frac{\mu V}{K}$ which is about two times greater than the theoretical value (Section 2.3.2). The deviation from theoretical thermopower value need to be further investigated, but the theoretical thermopower equation still provide a good estimation for the actual thermopower of the thermoelectrochemical cell.

3.3.2 pH Measurement and Calculation

The procedure for measuring pH has been explained in Section 3.2.2. Here, more detailed data for pH measurement will be presented in Table 4.

Table 3: Thermopower Processed Data

Corresponding Time Interval	Cold Side Temperature (Celsius)	Hot Side Temperature (Celsius)	Temperature Gradient (K)	Average Potential (V)
1107 sec - 1167 sec	22.5	62.8	40.3	-0.03181
1933 sec - 1993 sec	25.2	60.2	35.0	-0.02832
2760 sec - 2820 sec	27.8	57.8	30.0	-0.02411
3465 sec - 3525 sec	30.0	54.8	24.8	-0.01924
4274 sec - 4334 sec	32.4	52.5	20.1	-0.01514
5205 sec - 5265 sec	35.0	50.1	15.1	-0.01061
5799 sec - 5859 sec	37.8	47.9	10.1	-0.00614
6641 sec - 6701 sec	40.0	45.0	5.0	-0.00060
7206 sec - 7266 sec	42.5	42.5	0.0	0.00404

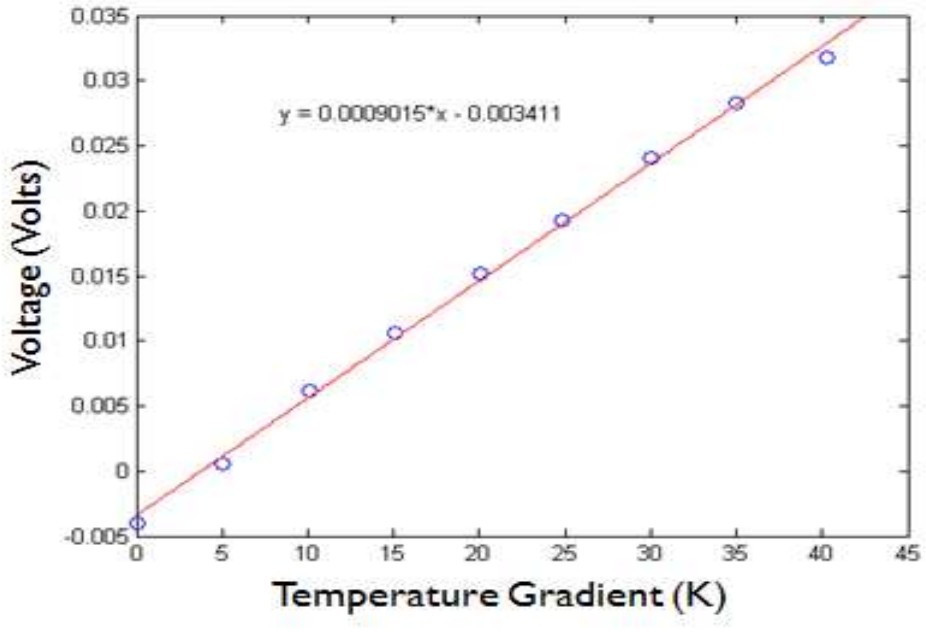

Figure 13: Thermopower (Seebeck-like Coefficient)

Table 4: pH Measurement Experimental Data

Temperature (Celsius)	Initial Buret Volume (ml)	Final Buret Volume (ml)	Change in Buret Volume (ml)	Number of mole of NaOH used	Number of mole of HNO3 in solution	H+ Concentration (M)	pH
22.0	1.65	26.66	25.01	0.15006	0.15006	15.006	-1.17626
31.0	3.75	28.70	24.95	0.14970	0.14970	14.970	-1.17522
40.5	3.95	28.85	24.90	0.14940	0.14940	14.940	-1.17435
53.0	3.20	27.90	24.70	0.14820	0.14820	14.820	-1.17085
61.5	3.10	27.30	24.20	0.14520	0.14520	14.520	-1.16197
70.0	11.90	36.05	24.15	0.14490	0.14490	14.490	-1.16107

The following provide sample calculation procedure for determining pH at 22 ℃:

Sample Calculation:

Chemical Reaction Equation in Titration:

$$HNO_3\ (aq) + NaOH\ (aq) \rightarrow NaNO_3\ (aq) + H_2O\ (l)$$

At 22℃:

Step 1: Change in Buret Volume = Final Buret Volume – Initial Buret Volume = 22.66 – 1.65 = 25.01 ml

Step 2: Number of Moles of NaOH used:

$$25.01\ ml * \frac{1\ L}{1000\ ml} * 6\ M = 0.15006\ mole$$

Step 3: Number of Mole of HNO_3 in Solution:

$$n_{HNO_3} \approx n_{NaOH} = 0.15006\ mole$$

Step 4: H^+ Concentration in Solution:

$$\frac{n_{HNO_3}}{10/1000} = 15.006\ M$$

Step 5: Calculate pH

$$pH\ (@T = 22℃) = -\log(15.006) = -1.176$$

Figure 14 plots the pH value using titration, theoretical calculation and pH meter measurement altogether. As it shows in Figure 14, pH measured using pH meter has a large deviation from theoretical calculation and titration, and the results from pH meter is irrational as the proton concentration increases in temperature range from 300 K to 340 K which is impossible as proton cannot be created from nowhere under the mass conservation condition.

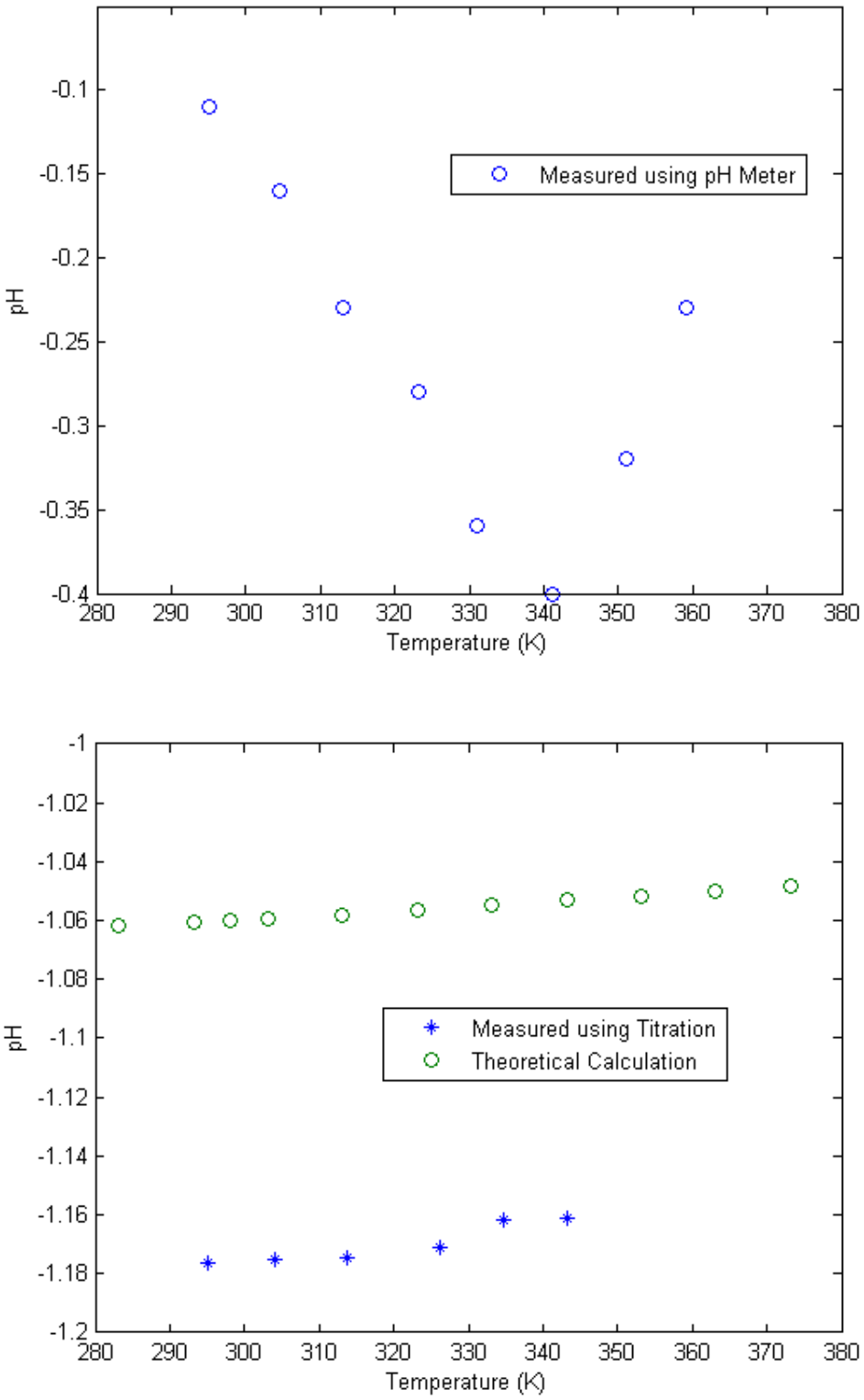

Figure 14: Comparison of pH Measurement with Different Methods

The pH results from titration was very consistent with the theoretical calculation both in tendency and pH values, and the pH values from titration will be adopted for calculating ZT (energy conversion efficiency) of the thermoelectrochemical cell. The difference between theoretical pH values and actual pH values measured using titration could resulted from that the actual molarity of nitric acid was a little deviated from 15 M due to manufacturing inconsistency from industry.

3.3.3 Electrical Conductivity Measurement

The measurement method for electrical conductivity has been explained in Section 3.2.2. Table 5 lists the electrical conductivity of thermoelectrochemical cell as different temperatures, and Figure 15 plots the results. As it shows in Figure 15, electrical conductivity does not vary with temperature significantly, and here it was assumed to be constant:

$$\sigma = 320\ mS/cm$$

in the operating temperature range of this research project for determining ZT.

Table 5: Electric Conductivity

Temperature (Celsius)	Electric Conductivity (mS/cm)
22	307
30	338
37	312
47	325
58	329
68	319

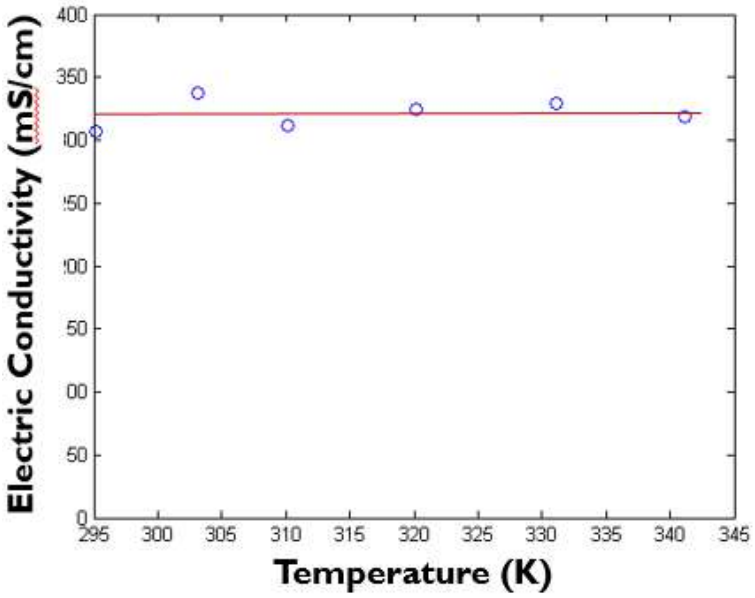

Figure 15: Electrical Conductivity

3.3.4 Power Calculation

The power of the thermoelectrochemical cell can be calculated using:

$$P = \frac{V}{R^2}$$

And the resistivity is the reciprocal of conductivity:

$$R = \frac{1}{\sigma}$$

If we take average value of conductivity here (as in Section 3.3.3):

$$\sigma = 320\ mS/cm$$

Therefore,

$$R = 3.125\ ohms/cm$$

The length of the channel is 10 cm:

$$R = 31.25\ ohms$$

in average of the entire temperature range. Then the power output of the thermoelectrochemical cell can be plotted in Figure 16 as a function of temperature:

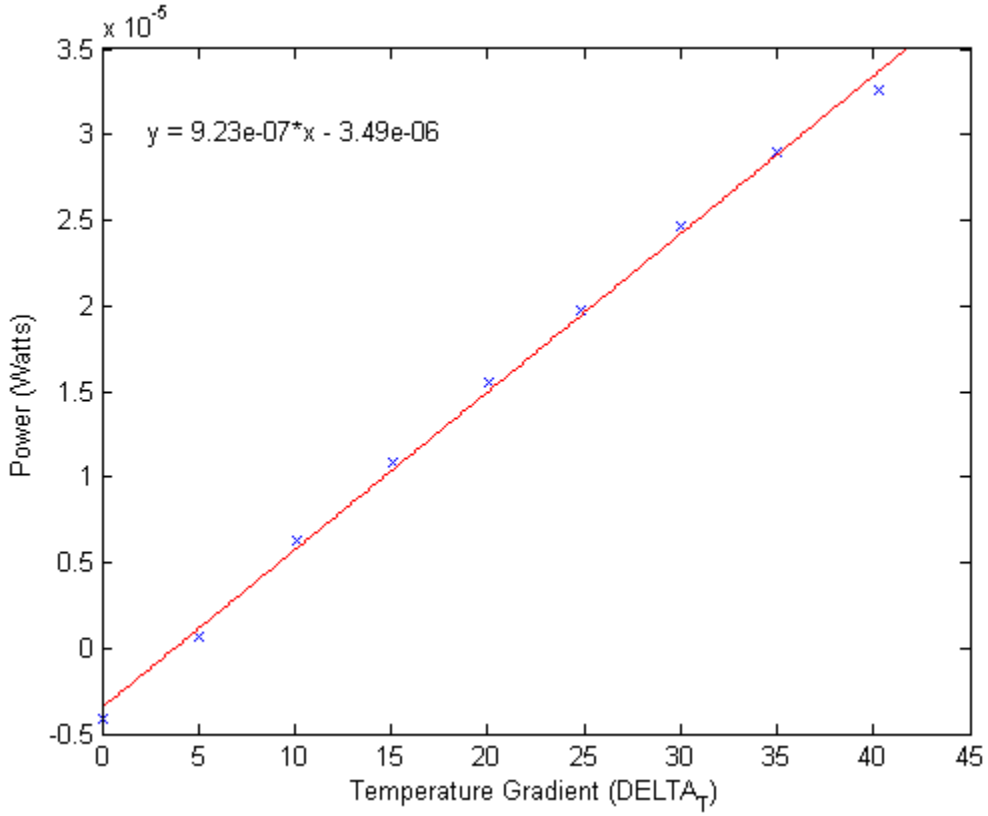

Figure 16: Power of Thermoelectrochemical Cell

3.3.5 Figure of Merit (ZT) Calculation

As mentioned in Section 1.2.2, the energy conversion efficiency of a thermoelectric material can be defined as:

$$ZT = \frac{\sigma S^2 T}{\lambda}$$

Here we have all the variables as a function of temperature except for thermal conductivity. The thermal conductivity of the electrolytes can be approximated as waters (Figure 17) [22].

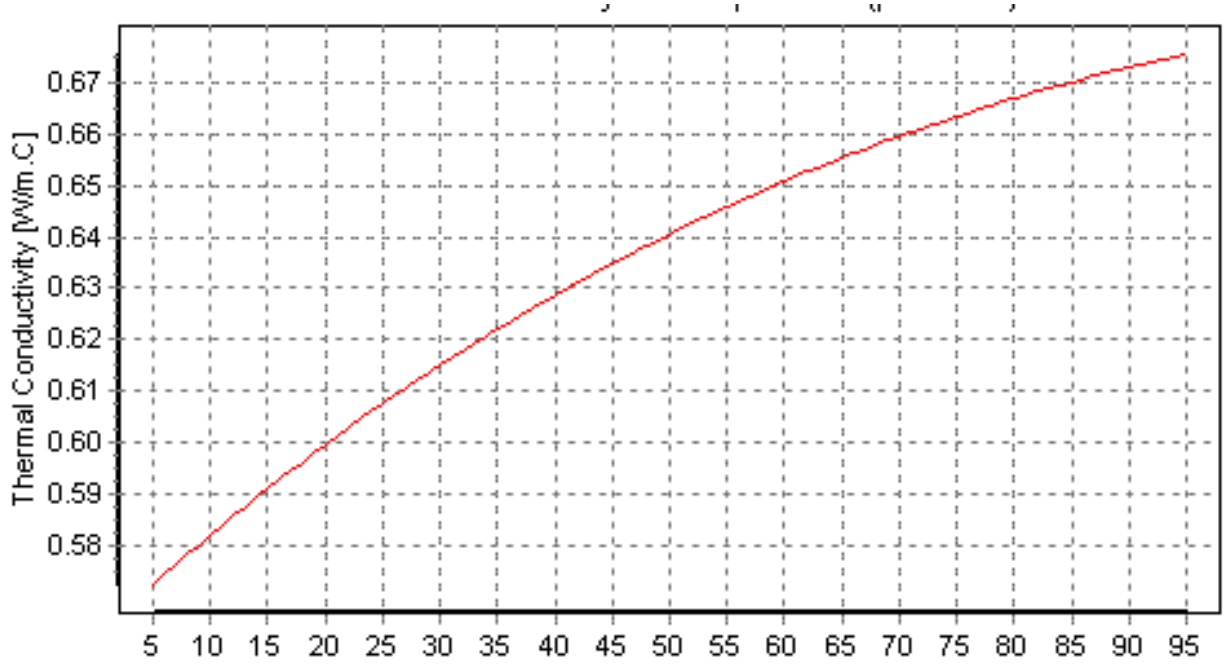

Figure 17: Thermal Conductivity of Water

Using the polynomial fit equation for water thermal conductivity given from the online resources [22]:

$$k(T) = -0.5752 + 6.397e-3T - 8.151e-6T^2 \left[\frac{W}{m}.K\right]$$

The ZT can be calculated and plotted in Figure 18:

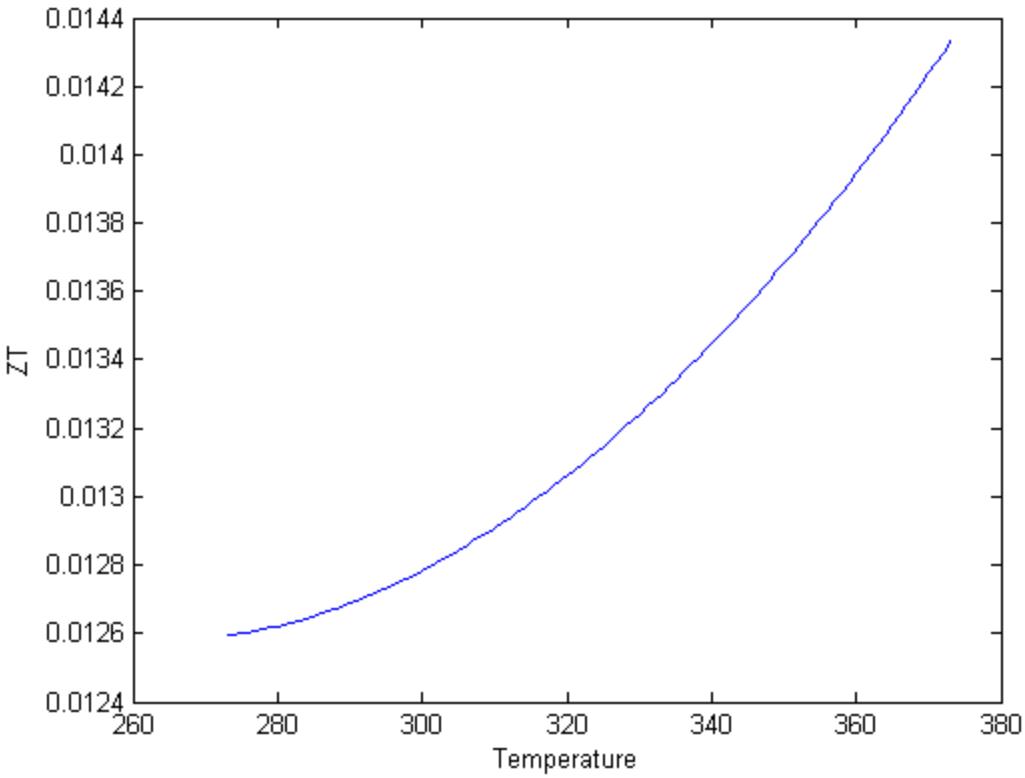

Figure 18: ZT of Thermoelectrochemical Cell

The ZT for this thermoelectrochemical cell gradually increase with temperature.

Chapter 4: Conclusion and Future Recommendations

The preliminary experiment was not designed to produce a high-efficiency thermoelectric converter, but merely to illustrate the existence of this new effect. The overall energy efficiency of this device will be characterized by a figure of merit ZT quite similar to that of solid-state devices,

$$ZT = \frac{\sigma S^2 T}{\lambda} \quad [9]$$

where λ is the thermal conductivity of the ionic conductor material or electrolyte. The average ZT of barium nitrate and nitric acid system is about 0.0134 in the temperature range from 295.5 K to 355.5 K. Compare to conventional solid-state thermoelectric materials, the new thermoelectrochemical cell does not have high energy conversion efficiency. However, the power output can be improved by just redesigning the geometry of the thermoelectrochemical cell (Figure 19) with large cross-section area and short connecting channel between two reaction cells.

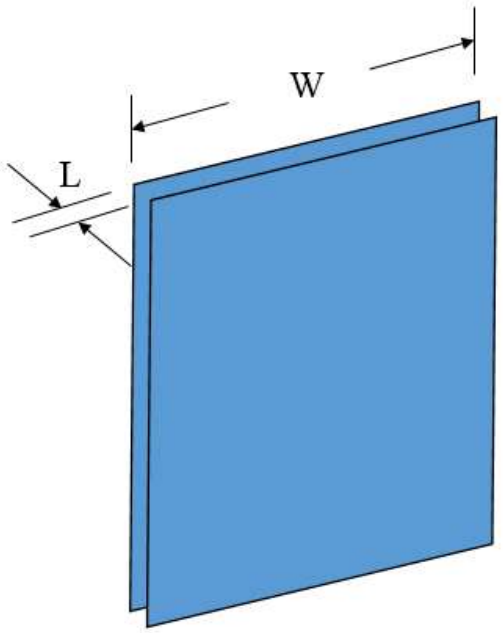

Figure 19: Proposed New Connecting Channel Design

In addition, the measured thermopower is about 901.5 $\frac{\mu V}{K}$ which is about two times greater the theoretical value (Section 2.3.2). The deviation from theoretical thermopower value need to be further investigated, but the theoretical thermopower equation still give a good estimation of the actual thermopower of the thermoelectrochemical cell.

An optimization process undergone by semiconductor thermoelectrics will need to be conducted in

this case [27]. The materials criteria are:

1. The electrochemical system must have charge carriers whose concentration is strongly temperature-dependent (maximize:

$$\frac{dln(n)}{dln(T)}$$

in (5)), for example by having the charge carriers arise from a chemical equilibrium reaction that is strongly *T*-dependent (solubility reactions of solids or gases in liquids, as shown, or thermally activated vacancies….)
2. The positively and negatively charged carriers must have different mobilities (protons/anions; Li ions/vacancies,….)
3. The numerator of *zT* is the power factor:

$$PF = \alpha^2\sigma$$

which depends on the charge carrier concentration *n*. In semiconductor thermoelectrics, there is one value of *n* that maximizes *PF*. Here, the relation:

$$\sigma = nezu$$

still holds, but the relation between

$$\frac{dln(n)}{dln(T)}$$

and *n* will be further investigated to elucidate that between *PF* and *n*.
4. The higher the ionic mobility, the better the *PF*. This is a disadvantage of thermoelectrochemical cells in general over semiconductor thermoelectrics. The extent to which the *PF* can be optimized and its eventual limitations compensated by geometrical effects and the low thermal conductivity is the subject of the proposed investigation.
5. In waste heat recovery applications, relevant temperatures for automotive applications are in the range of 100 t0 750 ^{o}C, in which case, aqueous solutions are not usable.

The following issues with the practical use of thermoelectrochemical cells will arise and will require engineering solutions at the macroscopic cell design.

1. Optimization of the cell geometry needs to take place and follow design rules similar to those used in solid thermoelectrics [27].
2. Liquids require containers. The containers will create thermal shorts which will conduct heat that does not do any useful work in the electrolyte. This again is a device optimization issue that can either be entirely avoided when using solid electrolytes, or minimized with engineering designs.
3. In mobile applications, the waste heat recovery cell is likely to be in a mechanically harsh environment and the material has to work in various positions.

References

[1] Chu, S., Majumdar, A. (2012). Opportunities and Challenges for a Sustainable Energy Future. *Nature*, 294-303.

[2] Estimated Energy Use in 2013. (2014). *Lawrence Livermore National Laboratory*.

[3] Bell, L. E. (2008). Cooling, Heating, Generating Power, and Recovering Waste Heat With Thermoelectric Systems. *Science*, 1457, 461.

[4] Biswas, K., Jiaqing H., Ivan D. B., Wu, C-I., Hogan T., Seidman D., Dravid, V., Kanatzidis, M. (2012) High-performance Bulk Thermoelectrics with All-scale Hierarchical Architectures. *Nature*, 414-18.

[5] Boretti, A. (2012) "Recovery of Exhaust and Coolant Heat with R245fa Organic Rankine Cycles in a Hybrid Passenger Car with a Naturally Aspirated Gasoline Engine." *Applied Thermal Engineering*, 36, 73-77.

[6] Organic Rankine Cycle Waste Heat Power Generation. (2012). *Pratt & Whitney Power Systems ORC Solutions*. Retrieved March 19, 2015.

[7] General Principles and Basic Considerations. (2006). In D. Rowe (Ed.), *Thermoelectrics Handbook: Macro to Nano* (pp. 1-2). New York: Taylor & Francis Group.

[8] Heremans, J. (2014). The ugly duckling. *Nature*, 508, 327-328.

[9] Callister, W., & Rethwisch, D. (2010). Electrical Properties. *In Material Science and Engineering: An Introduction* (8th ed., pp. 719 - 748). John Wiley & Sons.

[10] Callister, W., & Rethwisch, D. (2010). Thermal Properties. *In Material Science and Engineering: An Introduction* (8th ed., pp. 789 - 790). John Wiley & Sons.

[11] Chen, G. (2005). Energy States in Solids. *In Nanoscale Energy Transport and Conversion: A Parallel Treatment of Electrons, Molecules, Phonons, and Photons* (1st ed., pp 97). Oxford.

[12] Heremans, J., Dresselhaus, M., Bell, L., & Morelli, D. (2013). When Thermoelectric Reached the Nanoscale. *Nature Technology*, 8, 471-473.

[13] Yang, Y., Lee, S.W., Ghasemi, H., Loomis, J., Li, X.B., Kraemer, D., Zheng, G.Y., Cui Y., and

Chen, G. (2014) Charging-free Electrochemical System for Harvesting Low-grade Thermal Energy. *Proceedings of the National Academy of Sciences USA*, 111, 17011.

[14] Lee, S. W., Yang, Y., Lee, H-W., Ghasemi, H., Kraemer, D., Chen, G and Cui, Y. (2014). An Electrochemical System for Efficiently Harvesting Low-grade Heat. *Nature Communications* 5, 3942.

[16] Quickenden, T. I., and Mua, Y. (1995). A Review of Power Generation in Aqueous Thermogalvanic Cells. *J. Electrochem. Society*, 142, 3985.

[17] Callen, H.B. (1960) Thermodynamics, John Wiley & Sons, New York.

[19] Chen, G. (2005). *Nanoscale energy transport and conversion: A parallel treatment of electrons, molecules, phonons, and photons*. New York: Oxford University Press.

[20] Covington, A., Bates, R., & Durst, R. (n.d.). Definition of pH scales, standard reference values, measurement of pH and related terminology (Recommendations 1984). *Pure and Applied Chemistry*, 531-542.

[21] Young, R., & Horne, R. (1967). Electrical Conductivity of Aqueous 0.03 to 4.0 M Potassium Chloride Solutions under Hydrostatic Pressure. *The Journal of Physical Chemistry*.

[22] Syeilendra, P. (1997, January 1). Water Thermodynamic Properties. Retrieved January 1, 2015.

[23] General Principles and Basic Considerations. (2006). In D. Rowe (Ed.), *Thermoelectrics Handbook: Macro to Nano* (pp. 1-5). New York: Taylor & Francis Group.

[24] Thermoelectric Engineering. (2014). Thermoelectrics. *Caltech Materials Science*.

[25] Hsu, K. F. (2004). Cubic AgPbmSbTe2 M: Bulk Thermoelectric Materials with High Figure of Merit. *Science*, 818, 21.

[26] Heremans, J., Jovovic V., Toberer, E.S., Saramat, A., Kurosaki, A., Charoenphakdee, A., Yamanaka, S., and G. J. Snyder. (2008). Enhancement Of Thermoelectric Efficiency In PbTe By Distortion Of The Electronic Density Of States. *Science*, 321, 554-557.

[27] Heikes, R., & Ure, R. (1961). *Thermoelectricity: Science and engineering*. New York: Interscience.